

RSC Advances



This is an *Accepted Manuscript*, which has been through the Royal Society of Chemistry peer review process and has been accepted for publication.

Accepted Manuscripts are published online shortly after acceptance, before technical editing, formatting and proof reading. Using this free service, authors can make their results available to the community, in citable form, before we publish the edited article. This *Accepted Manuscript* will be replaced by the edited, formatted and paginated article as soon as this is available.

You can find more information about *Accepted Manuscripts* in the [Information for Authors](#).

Please note that technical editing may introduce minor changes to the text and/or graphics, which may alter content. The journal's standard [Terms & Conditions](#) and the [Ethical guidelines](#) still apply. In no event shall the Royal Society of Chemistry be held responsible for any errors or omissions in this *Accepted Manuscript* or any consequences arising from the use of any information it contains.

Preparation of Graphene Oxide Nano-composite Ion-exchange Membranes for Desalination Application

Swati Gahlot^a, Prem P. Sharma^a, Hariom Gupta^a, Vaibhav Kulshrestha^{ab*}, Prafulla K Jha^c

^a*CSIR-Central Salt and Marine Chemicals Research Institute (CSIR-CSMCRI), Council of Scientific & Industrial Research (CSIR), Gijubhai Badheka Marg, Bhavnagar- 364 002, (Gujarat), INDIA
Fax: +91-0278-2566970.
E-mail: vaibhavk@csmcri.org, vaihavyphy@gmail.com*

^b*Academy of Scientific and Innovative Research, CSIR-Central Salt and Marine Chemicals Research Institute (CSIR-CSMCRI), Council of Scientific & Industrial Research (CSIR), Gijubhai Badheka Marg, Bhavnagar- 364 002, (Gujarat), INDIA*

^c*Department of Physics, The M S University of Baroda, Vadodara, (Gujarat), INDIA*

Abstract

Nano-composite ion-exchange membranes (IEMs) consisting of graphene oxide (GO) (0.5, 1, 2, 5 and 10%) (w/w) and sulfonated polyethersulfone (SPES) of thickness 180 μm are prepared with enhanced electrochemical properties. In particular, the transport properties of SPES are favourably manipulated by the incorporation of GO. Intermolecular interactions between the components in composite membranes are established by FTIR. Membranes are characterized by transmission electron microscopy (TEM) and scanning electron microscopy (SEM) which showed the uniform distribution of GO sheets in SPES matrix. The maximum ionic conductivity has been found in 10% GO composite with higher methanol crossover resistance and selectivity. Water desalination performance of the nano-composite membranes have been evaluated by ionic flux, power consumption and current efficiency during salt removal. 10% GO nano-composite membrane shows 3.51 mole $\text{m}^{-2} \text{h}^{-1}$ ionic flux, 4.3 kWh kg^{-1} power consumption and 97.4% current efficiency for salt removal. The values of ionic flux and current efficiency are 19% & 12% higher respectively while 20% lower power consumption is observed as compared to SPES membrane. The strong interfacial interactions due to the insertion of GO nanofillers into the SPES matrix improve the thermal and mechanical properties of the nanocomposite membranes. Nano-composite membrane shows the better performance and higher stability which may be used for the practical application such as DMFC and electro dialysis.

Keywords: SPES; Graphene Oxide; PEMs; Water desalination

Introduction:

Energy and fresh water are demands on priority of today's world. Researchers are constantly developing techniques to fulfill such requirements. Fuel cell technology is one of the best alternate of conventional energy generation methods. Polymer electrolyte membrane fuel cells (PEMFC) are devices with advantage of high power density and better efficiency [1-4]. Electrodialysis is a process for removal of ions from brackish or sea water to produce fresh water including waste water treatment to recover some valuable elements in chemical industry [5-7]. Both the processes employ ion exchange membrane (IEM). IEMs for electrodialysis and fuel cell must exhibit high ionic conductivity, high permselectivity for counter ions, high chemical stability and low fuel permeability [8, 9]. Different types of membranes have been developed suitable for above applications using several polymer/organic or inorganic material. Such kinds of membranes own the better physiochemical properties and also incorporate the advantages of membrane forming attribute of polymers [10, 11]. Different materials that are being used for nanocomposite membranes are silica, carbon nanotubes, graphene oxide etc. Composites of polymers with Carbon nanotubes (CNT) have been reported for water treatment application [12]. Vertically aligned CNTs has also been utilized to measure desalination efficiency under pressure driven conditions [13]. SPEEK/silica membrane has been reported for direct methanol fuel cell (DMFC) application and shows better performance [14]. Thus incorporation of organic or inorganic material into polymer matrix not only enhanced the properties but also expand the application region. Graphene Oxide (GO) is emerging as an efficient material whose composite with polymer can be utilized for many applications such as biosensors, super capacitors, fuel cell etc [15-17]. The fascinating properties of GO e.g. high surface area, excellent mechanical strength etc. makes it a distinct material to be used as organic filler for nanocomposite membrane [18-19]. Poly (ethylene oxide) (PEO)/GO electrolyte membrane was prepared by Cao et. al. for low temperature fuel cell [20]. Polysulfone/GO membrane with enhanced hydrophilicity was prepared by B. M. Ganesh et. al. and used for rejection of salts from water [21].

Herein, we demonstrate the fabrication of SPES/GO composite membrane for fuel cell and electrodialysis application. Membranes containing various weight content of GO (n=0.5, 1, 2, 5 and 10%) are prepared and designated as SG-n. Physical and electrochemical characterizations of prepared membranes are made using different techniques. Investigations of ion exchange capacity (IEC), water uptake are done and their performance towards water desalination is presented in manuscript.

Experimental:***Materials and Methods:***

Graphite powder is purchased from Sigma Aldrich. Poly(ether-sulfone), obtained from Solvay chemicals, India, is used after drying under vacuum. Other chemicals are obtained commercially and used as received without further purification.

Graphene oxide is prepared using modified Hummer's Method [17]. Typically in a round bottom flask 1gm graphite, 1gm NaNO_3 and 46 ml H_2SO_4 are taken and stirred for 2 hour in an ice bath at $0-5^\circ\text{C}$. 8 gm KMNO_4 was added in above solution with stirring at room temperature for 4 hour. Now 80 ml water is added drop wise with stirring for 3 hour as it produces enormous amount of heat. Finally, 200 ml water and 5% H_2O_2 is added and washed repeatedly and centrifuged to recover GO. Sulfonation of PES was carried out as reported earlier using conc. H_2SO_4 (95–98%) [22]. Known amount of GO is dissolved in N-N' dimethylacetamide and sonicated for 3-4 hour for uniform dispersion. Definite quantity of SPES polymer is dissolved in the GO solution with stirring for 4 hours followed by further sonication for 6 h. Resulting solution was cast on glass followed by vacuum drying. Membranes with different GO concentration (0, 0.5, 1, 2, 5 and 10 %) (w/w) are prepared and designated as SPES, SG-05, SG-1, SG-2, SG-5 and SG-10 respectively. The schematic representation for graphite to composite membrane preparation is shown in Scheme 1. Polyethylene based styrene divinylbenzene anion exchange membrane is used for the study. The detail for membrane preparation is included in the supplementary information section.

Characterization of the membranes:

The membranes are characterized by the means of chemical, structural, mechanical, thermal and electrochemical using different techniques. Details are included in the Electronic Supplementary Information (ESI) section.

Ionic and electronic conductivity of the membranes:

Ionic conductivity measurements of the composite membranes are conducted on a potentiostat/galvanostat frequency response analyzer (Auto Lab, Model PGSTAT 30) in water at different temperatures ranging from 30 to 90°C . Before measurements all the membranes are fully equilibrated with water. For the measurement the membranes are sandwiched between two

circular stainless steel electrodes (1.0 cm^2). The membrane resistances were obtained from Nyquist plots and the ionic conductivity (σ) was calculated from equation [23]:

$$\sigma (\Omega^{-1} \text{ cm}^{-1}) = \frac{L (\text{cm})}{R (\Omega) \times A (\text{cm}^2)}$$

where L is the distance between the electrodes used to measure the potential, R is the resistance of the membrane, and A is the surface area of the membrane.

The electronic conductivity of the dry membranes was measured with Keithley electro meter using following equation:

$$\sigma (\Omega^{-1} \text{ cm}^{-1}) = \frac{G (\text{S}) l (\text{cm})}{A (\text{cm}^2)}$$

where l is the thickness of membrane, G is the conductance of the membrane, and A is the surface area of the membrane.

Methanol crossover resistance:

Resistance to methanol crossover for the membranes are evaluated by the measurement of the methanol permeability with two compartment cell. Details of the experiment and formula used are described in Electronic Supplementary Information (ESI) section.

Desalination by electrodialysis:

The performance of the prepared membranes is tested in a locally fabricated PVC based ED cell. The effective area of the membranes during ED was 60 cm^2 . The scheme of the ED setup and the membrane configuration in the cell are illustrated in Scheme 2, which consists of five compartments. Precious titanium oxide based electrodes was used as cathode and anode. A DC power source was used to apply constant potential across the electrodes and resulting current was recorded using a Aplab L1285 power supply. During ED 600 cm^3 of 0.1 mol dm^{-3} NaCl feed solution was re-circulated at 3 L/h through the dilute (DC) and concentrated compartments (CC). The CC was adjacent to the electrode wash (EW) compartments in which 500 cm^3 of 0.1 mol dm^{-3} Na_2SO_4 was circulated at 3 L/h. The ion concentration from each compartment was determined by a conductivity and pH measurements of the DC and CC during the ED process. The volume change in each reservoir was also recorded during the experiment. The performances of the prepared membranes were analyzed in terms of flux, current efficiency and energy consumption calculated by the following equations [6];

$$Flux = \frac{V(C_0 - C_t)}{At} \quad (1)$$

$$P(kWhkg^{-1}) = \frac{1}{m} \int UI dt \quad (2)$$

$$\eta = \frac{FnV(C_0 - C_t)}{n_c \int I dt} \times 100 \quad (3)$$

where η is the current efficiency, F is Faraday constant, V is the volume of the dilute (dm^3), C_0 and C_t are the concentration of dilute compartment at zero time and time t , A is the effective membrane area, P is the power consumption, n is the stoichiometric number ($n = 1$ for NaCl), n_c is the number of cell pair, U is the applied voltage and I is current (A).

Results and discussion:

Structural and chemical characterization:

The graphite is converted into the GO by modified Hummer's methods and confirmed by the XRD and FTIR analysis. XRD spectra of GO showed the diffraction peak at 11.31° while diffraction peak for graphite appeared at 26.05° well matched with the literature (Fig. 1)[24, 25]. The interlayer spacing of GO increased by 7.81 \AA to the initial value 3.4 \AA for graphite. Also it can be seen from the fig that peak shifts towards left and becomes broader which is due to the addition of functional groups at GO. The presence of a range of reactive groups such as carboxyl, hydroxyl, epoxy etc. on GO can be confirmed by FTIR analysis as shown in Fig. 2. FTIR spectra of prepared GO shows O-H stretching at 3402 cm^{-1} , C=O stretching at 1717 cm^{-1} , 1624 cm^{-1} and C-O stretching at 1051 cm^{-1} [25]. The presence of sulfonic acid groups in PES is confirmed by the FTIR analysis and the degree of sulfonation is found to be 60-65 % as confirmed by $^1\text{H NMR}$ [26]. The interaction between polymer and GO is also determined by FTIR spectra. Fig. 2 illustrates the FTIR spectra of SPES and SG-10 membranes. The addition of functional groups is more in SG-10 as compared to the SPES. This is due to the presence of GO in SG-10 membrane which adds reactive groups onto the membrane matrix. XRD diffraction graphs of SPES and SG-10 membrane are shown in Fig. S-1. The diffraction peak for SPES and SG-10 membrane are

found to be at 22.21° and 17.96° respectively, the shift in peak is due to the presence of GO in SPES matrix.

Fig. 3 shows the AFM, SEM and TEM images of GO. All three analysis shows that GO have the flakes like structure. Fig. 4 (A, B & C) shows the 3 dimensional AFM images of prepared membranes. Surface roughness of each membrane was calculated using NT-MDT software which varies from 6.5 nm to 24.35 nm for SPES and SG-10 membrane respectively. Thus it reveals the increasing roughness value of membranes with increasing the amount of GO. Fig. 4 (D, E, F & G) shows the SEM images of SPES, SG-1, SG-5 and SG-10 membranes. Cross-sectional views of composite membranes demonstrate layered structure of dispersed GO sheets into the SPES matrix. TEM images of GO composite membranes at different magnifications are shown in Fig. 4 (H, I & J). The transparency of images shows the interaction between SPES and GO, and the uniform dispersion of GO into the SPES matrix (Fig. 5).

Thermal and mechanical characterization:

Characterization of thermal properties of GO and nanocomposite membranes was done by using TGA. Fig S-2 shows the TGA and DTG curve for GO powder. Three step weight losses can be observed from the graph at 85, 215 and 293°C (as obtained from DTG curve). Fig S-3 demonstrates the TGA and DTG graphs of composite membranes respectively. As obtained by DTG graphs the maximum degradation temperature was found to be between $500\text{--}600^\circ\text{C}$. Other two weight losses are observed in the range from $200\text{--}300^\circ\text{C}$ and $400\text{--}450^\circ\text{C}$ respectively. There is a gradual decrease in the thermal stability of membranes as the amount of GO increases which may be due to the presence of carboxyl and hydroxyl groups on GO's surface. The change from 200 to 300°C is attributed to the degradation of functional groups present in membrane [22]. Thermal degradation from 500 to 600°C can be described by decomposition of the back bone of polymer chains. DSC graphs of GO composite membranes are shown in Fig S-4 for all the prepared membranes. The melting peak of composite membranes shifts towards the higher temperature side by incorporating the GO amount into the SPES matrix. The thermo-mechanical studies of composite membranes are performed by DTMA analysis as shown in Fig. S-5. Fig. shows that the storage modulus and temperature of $\text{Tan}(\delta)$ increases by increasing the GO content into the membrane [27, 28]. The GO flakes are working as the fillers for SPES matrix and decreasing the pore size of the membrane, which provide the higher mechanical as well as thermal stability.

Electrochemical properties:

Water uptake (WU), dimensional stability (DS) and IEC are important parameter for ion exchange membrane. Table 1 show the WU, DC and IEC values of each membrane. The IEC of the composite membrane decreases slightly due to GO content into the membrane matrix and approached to 1.27 meq./gm [18]. The presence of carboxyl, hydroxyl group in the GO maintain the IEC of the membranes. As can be seen from the table, WU increases from lower to higher GO concentration (from SPES to SG-10). SG-10 (10% GO) shows the maximum water uptake i.e. 15.19%. The important factor of the membrane is swelling, which decreases by incorporating the GO content in the SPES. This may be due to the reduction of pore size in the membrane as GO is acting as the filler. The bound water into the membrane is found to be increased by GO content, as calculated by TGA analysis of the membrane between 100-150 °C. SPES membranes shows the lowest bound water content in comparison with all membranes while highest bound water in SG-10 composite membrane, more bound water in membrane maintain higher water retention ability.

Ionic and electronic conductivity:

In Table 1 the values of ion conductivities are shown for different membranes. The ionic conductivities of composite membranes are calculated by Nyquist plot. In the ionic conductivities of the GO/SPES membranes, with the GO particles introduced into the SPES matrix, the ionic conductivity of the GO/ SPES membranes was increased regardless of the amounts of GO particles [29, 20]. The increment in the conductivity is due to the presence of carboxyl and hydroxyl groups present in GO particles. The effect of temperature on ionic conductivity is studied from 30 to 90°C, on increasing the temperature the conductivity of the membranes also increases due to the higher ionic diffusion at higher temperature as shown in Fig. 6. Electronic conductivity of the composite membranes decreases as the GO content increases in SPES matrix. SG-10 membrane has the lowest value. Since addition of GO increases the insulating groups to the membranes but at higher concentration agglomeration occurs which prevents higher electronic conductivity of the composite membranes as shown in Table 1.

Methanol permeation (P_M) resistance and selectivity of hybrid membranes:

Low methanol permeation with high proton conductivity is the basic requirement for proton exchange membrane for DMFC application. Methanol permeability of SPES and GO/SPES

membranes is shown in Fig. 7. It can be seen that the methanol permeability of composite membrane decreased with increment of GO content. The GO is acting as the blocking agent for methanol and reducing the free volume of the composite membranes [18]. The interaction between GO and SPES restricts the formation of the channels in membranes, which leads to low methanol permeability. The methanol permeability for the SPES membrane is found to be $1.827 \times 10^{-7} \text{ cm}^2\text{S}^{-1}$, which reduces to $1.44 \times 10^{-7} \text{ cm}^2\text{S}^{-1}$ for SG-1 and $1.412 \times 10^{-7} \text{ cm}^2\text{S}^{-1}$ for SG-5 membranes. Finally the methanol permeability value for SG-10 reached to $1.345 \times 10^{-7} \text{ cm}^2\text{S}^{-1}$. We also calculate the selectivity of the membrane. For the SPES it is found to be 1.724×10^5 , which enhanced in composite membranes and further reached to 6.321×10^5 for SG-10 membrane. The low methanol permeability and high selectivity of SG-10 membrane makes it applicable for fuel cell.

Electrodialytic performance of composite ion exchange membranes:

Current-Voltage (*i-v*) characteristics for different composite membranes are studied in equilibration with 0.1 M NaCl solution and depicted in Fig. 8. The *i-v* curves shows three typical characteristic regions, viz., Ohmic, plateau and non-Ohmic which reveal the information about the ion transport and concentration polarization phenomenon across the ion-exchange membranes [30, 31]. In ohmic region the current density increases with applied potential due to presence of large number of ions, in plateau region current density remains constant with applied potential and in non-ohmic region or over-limiting region ions get depleted causing water splitting and high current density. ΔV (plateau length), Δi , and I_{lim} values for composite membranes are calculated from Fig. 8 and presented in Table 2 [31]. For SPES/GO membranes the plateau length and Δi values increases with the increase in GO content. Relatively higher ΔV and Δi values for membranes with high fixed charge concentration indicates their high electro-transport of counter ions from the diffusive boundary layer to the membrane matrix and thus results in higher current for concentration polarization (I_{lim}). The transport of counter ions through an ion-exchange membrane leads to the difference in counter ion concentration on the two membrane surfaces, which in turn creates concentration polarization [32]. The SG-10 membrane shows superior electro-transport properties and can be used for the water desalination. Electro-dialysis (ED) experiments are performed to assess the suitability of the developed membranes for the water desalination. Experiments were performed at constant applied potential (2.0 V/Cell pair) using 0.1 mol dm^{-3} NaCl solution as feed for both of DC and CC and Na_2SO_4 solution (0.1 mol dm^{-3}) through both electrode rinse compartments, in the recirculation mode.

The suitability of developed membranes for desalination applications are assessed in terms of estimating current efficiency and energy consumption for salt removal. Variation in current with time during the ED experiment for different membranes is presented in Fig. 9(A). Current at the constant applied potential decreases with time as the ions migrate from DC to CC as shown in figure. The time versus concentration profile for DC during electro dialysis is shown in figure Fig. 9(B). The concentrations of DC depleted with time in the linear fashion. The concentration of DC depleted faster with SG-10 membrane than other due to its higher ionic conductivity that facilitate the transport of ions from one compartment to another. The concentration of DC decreases from $0.1 - 0.009 \text{ mol dm}^{-3}$ in 118 minute with SG-10 membrane while it takes 160 minute time with SPES membrane for same concentration (Fig. 9(B)). The change in the conductivity of DC and CC are shown in Fig. 9(C), as conductivity of DC decreases its increases for CC. The decrement in conductivity of DC with SG-10 membrane is faster than SPES due to its higher ionic conductivity. No remarkable change is recorded in pH during electro dialysis experiments.

Flux for NaCl migration from DC can be obtained by equation 1, considering negligible mass (water) transport through membranes. Table 3 shows the NaCl flux for different composite membranes at constant potential. Ionic flux across the composite membranes followed the trend: SG-10 > SG-5 > SG-2 > SG-1 > SPES. This observation suggested that the rate of ion transport across SG-10 is higher than others. Table 3 shows the power consumption and current efficiency data to evaluate the performance of composite membranes. It is observed that P decreased, while CE increased with the increase in GO content in the membrane matrix. Efficiency parameters (J , P and CE) depend on operating conditions of ED cell as well as nature and electrochemical properties of membranes. The CE and P for the SG-10 membrane are found to be 97.4% and 4.30 kWh kg⁻¹ respectively, while 87.1% and 5.4 kWh kg⁻¹ for SPES membrane which shows the potential of the composite membrane for electrochemical devices.

Conclusion:

Graphene oxide nano sheet of $0.264 \mu\text{m}^2$ have been successfully synthesised by modified Hummer's methods. The elastic modulus value for SG-10 composite membrane is found to be 2.9 GPa, which is 35% higher than SPES membrane similarly 16 % gain is observed in glass transition temperature which is $240 ^\circ\text{C}$ for SG-10. The increase in ionic conductivity with temperature measurements revealed that GO did not affect the phase separated morphology or the ion conduction mechanism, which is also supported by thermo gravimetric analysis. The high

ionic conductivity of the GO/SPES nano-composite membrane is from the chemical interactions between GO/SPES, and also the presence of different oxygen functionalities on GO, which markedly enhanced ionic transport. Fig. 10 summarized the influence of GO on different membrane properties relevant for electrochemical application. SG-10 composite membranes demonstrated the highest ionic conductivity and selectivity that is $6.4 \times 10^{-2} \text{ Scm}^{-1}$ and $6.27 \times 10^5 \text{ cm}^2 \text{ S}^{-1}$ respectively. The value for ionic conductivity is 2.74 times and selectivity is five times higher than that of SPES which are $2.34 \times 10^{-2} \text{ Scm}^{-1}$ and $1.28 \times 10^5 \text{ cm}^2 \text{ S}^{-1}$ respectively. The power consumption and current efficiency values during salt removal using SG-10 membrane are calculated to be 4.3 kWhkg^{-1} and 97.4% respectively while ionic flux across the membrane is calculated to be $3.51 \text{ mole m}^{-2} \text{ h}^{-1}$. Power consumption is 20% lower and 12 % higher current efficiency is achieved compared to SPES membrane. According to the results the nano-composite membrane is highly stable and shows the higher ionic transport efficiency. Incorporation of GO in SPES is confirmed to be excellent scheme to enhance the transport and mechanical properties of SPES membranes.

ACKNOWLEDGEMENTS

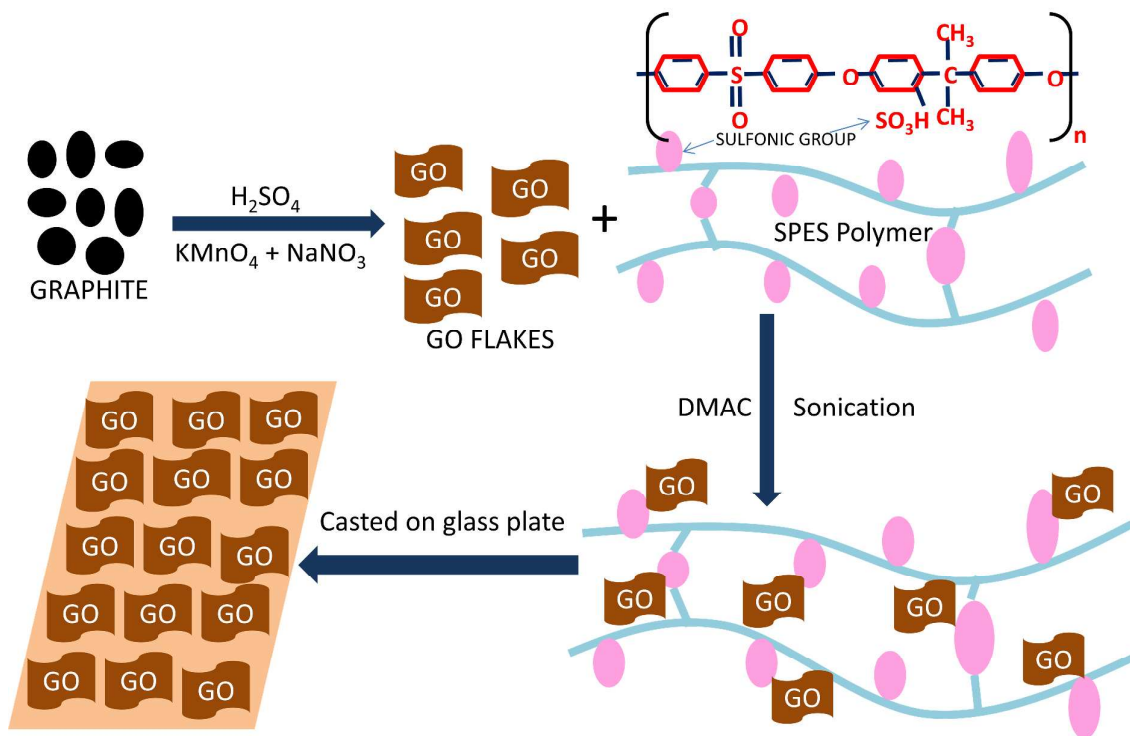
CSIR-CSMCRI communication number: 051/ 2014.

Authors are grateful to Department of Science and Technology, New Delhi, for sponsoring of project no. DST/TM/WTI/2k10/244/A. Instrumental support received from Analytical Science Division, CSIR-CSMCRI is gratefully acknowledged.

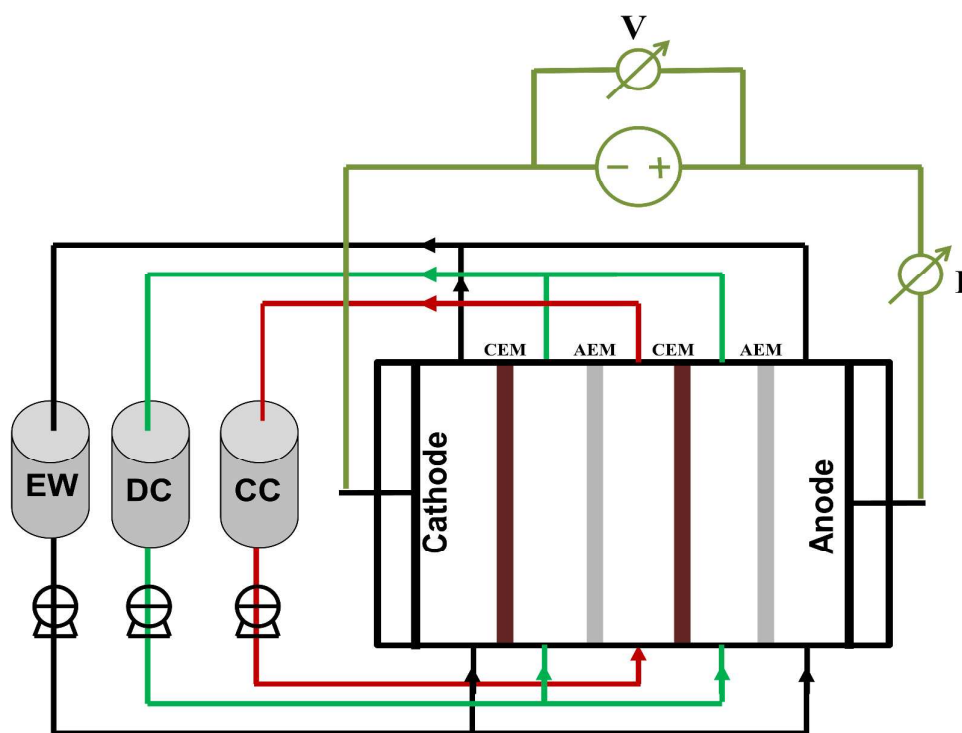
References:

1. Miyatake, K.; Tombe, T.; Chikashige, Y.; Uchida, H.; Watanabe, M.. *Angewadte Chemie Int. Ed.* **2007**, *46*, 6646.
2. Lin, H. L.; Wang, S. H. *J. Mem. Sci.* **2014**, *452*, 253.
3. Omosebi, A.; Besser, R. S. *J. Power Sources* **2013**, *228*, 151.
4. Tripathi, B. P.; Schieda, M.; Shahi, V. K.; Nunes, S. P. *J. Power Sources* **2011**, *196*, 911.
5. Chakrabarty, T.; Rajesh, A. M.; Jasti, A.; Thakur, A. K.; Singh, A. K.; Prakash, S.; Kulshrestha, V.; Shahi, V. K. *Desalination* **2011**, *282*, 2.
6. Nataraj, S.K.; Sridhar, S.; Shaikha, I. N.; Reddy, D.S.; Aminabhavi, T.M. *Sep. Puri. Tech.* **2007**, *57*, 185
7. Nataraj, S.K.; Hosamani, K. M.; Aminabhavi, T.M. *Desalination* **2007**, *217*, 181
8. Choi, B. G.; Hong, J.; Park, Y. C.; Jung, D. H.; Hong, W. H.; Hammond, P. T.; Park, H. S. *ACS Nano* **2011**, *5*, 5167.
9. Peighambardoust, S. J.; Rowshanzamir, S.; Amjadi, M. *Int. J. Hydrogen Energy* **2010**, *35*, 9349.
10. Klaysom, C.; Marschall, R.; Wang, L.; Ladewiga, B. P.; Max, Lu, G. Q. *J. Mater. Chem.* **2010**, *20*, 4669.
11. Burgaz, E.; Lian, H.; Alonso, R. H.; Estevez, L.; Kelarakis, A.; Giannelis, E. P. *Polymer* **2009**, *50*, 2384.
12. Celik, E.; Park, H.; Choi, H.; Choi, H. *Water Research* **2011**, *45*, 274.
13. Fornasiero, F.; Park, H. G.; Holt, J. K.; Stadermann, M.; Grigoropoulos, C. P.; Noy, A.; Bakajin, O. *Proceedings of the National Academy of Sciences* **2008**, *105*, 17250.
14. Roelofs, K. S.; Hirth, T.; Schiestel, T. *J. Mem. Sci.* **2010**, *346*, 215.
15. Choi, B. G.; Park, H. S.; Park, T. J.; Yang, M. H.; Kim, J. S.; Jang, S. Y. *ACS Nano* **2010**, *4*(5), 2910.
16. Zarrin, H.; Higgins, D.; Jun, Y.; Chen, Z.; Fowler, M. *J. Phys. Chem. C* **2011**, *115*, 20774.
17. Chen, D.; Feng, H.; Li, J. *Chem. Rev.* **2012**, *112* (11), 6027.
18. Tseng, C. Y.; Ye, Y. S.; Cheng, M. Y.; Kao, K. Y.; Shen, W. C.; Rick, J.; Chen, J. C.; Hwang, B. J. *Adv. Energy Mater.* **2011**, *1*, 1220.
19. Potts, J. R.; Dreyer, D. R.; Bielawski, C. W.; Ruoff, R. S. *Polymer* **2011**, *52*, 5.
20. Cao, Y. C.; Xu, C.; Wu, X.; Wang, X.; Xing, L.; Scott, K. *J. Power Sources* **2011**, *196*, 8377.
21. Ganesh, B. M.; Isloor, A. M.; Ismail, A. F. *Desalination* **2013**, *313*, 199.

22. Thakur, A. K.; Gahlot, S.; Kulshrestha, V.; Shahi, V. K. *RSC Advances* **2013**, *3*, 22014.
23. Li, J.; Park, J. K.; Moore, R. B.; Madsen, L. A. *Nature Materials* **2011**, *10*, 507.
24. Lee, D. W.; Los Santos, V. L. De; Seo, J. W.; Felix, L. L.; Bustamante, A. D.; Cole, J. M.; Barnes, C. H. W. *J. Phys. Chem. B*, **2010**, *114*, 5723.
25. Zeng, C.; Tang, Z.; Guo, B.; Zhang, L. *Phys. Chem. Chem. Phys.* **2012**, *14*, 9838.
26. Mondal, A. N.; Tripathi, B. P.; Shahi, V. K. *J. Mater. Chem.* **2011**, *21*, 4117.
27. Kulshrestha, V.; Agarwal, G.; Awasthi, K.; Tripathi, B.; Acharya, N. K.; Vyas, D.; Saraswat, V. K.; Vijay, Y. K.; Jain, I. P. *Micron* **2010**, *41*, 390.
28. Kulshrestha, V. *Int. J. Hydrogen Energy* **2009**, *34*, 9274.
29. Kumar, R.; Xu, C.; Scott, K. *RSC Advances* **2012**, *2*, 8777.
30. Singh, S.; Jasti, A.; Kumar, M.; Shahi, V. K. *Polym. Chem.* **2010**, *1*, 1302.
31. Kumar, M.; Singh, S.; Shahi, V. K. *J. Phys. Chem. B* **2010**, *114*, 198.
32. Strathmann, H. Electrodialysis. In *Membrane Separations Technologys Principles and Applications*; Noble, R. D., Stern, S. A., Eds.; Elsevier Press: Ireland, **1995**.



Scheme 1: Schematic representation for graphite to composite membrane preparation



Scheme 2: Schematic representation of the ED system and cell configuration

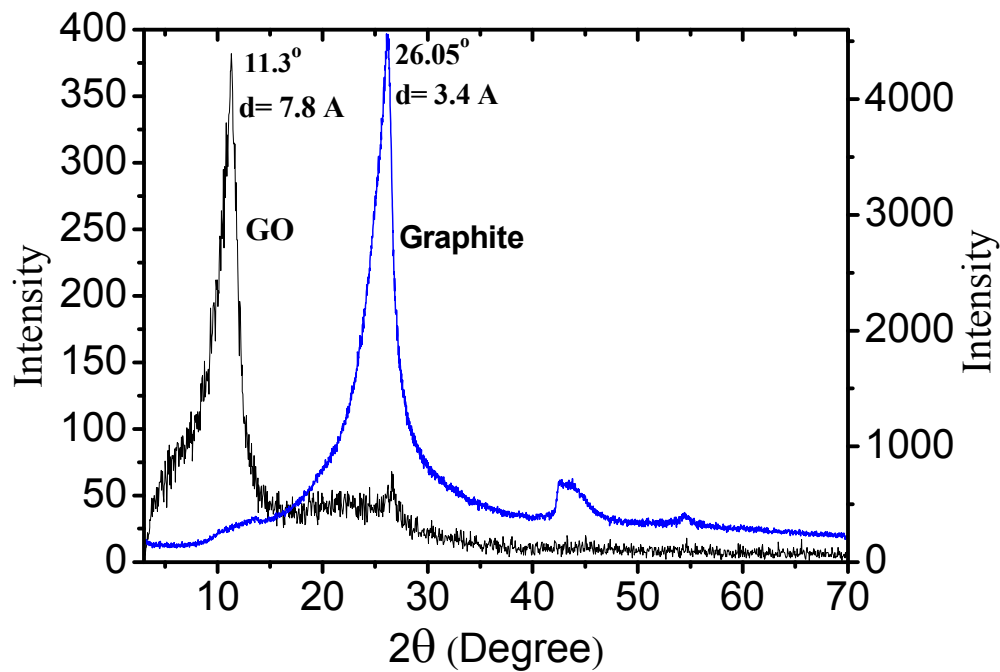


Fig.1: XRD patterns for Graphite and Graphene Oxide

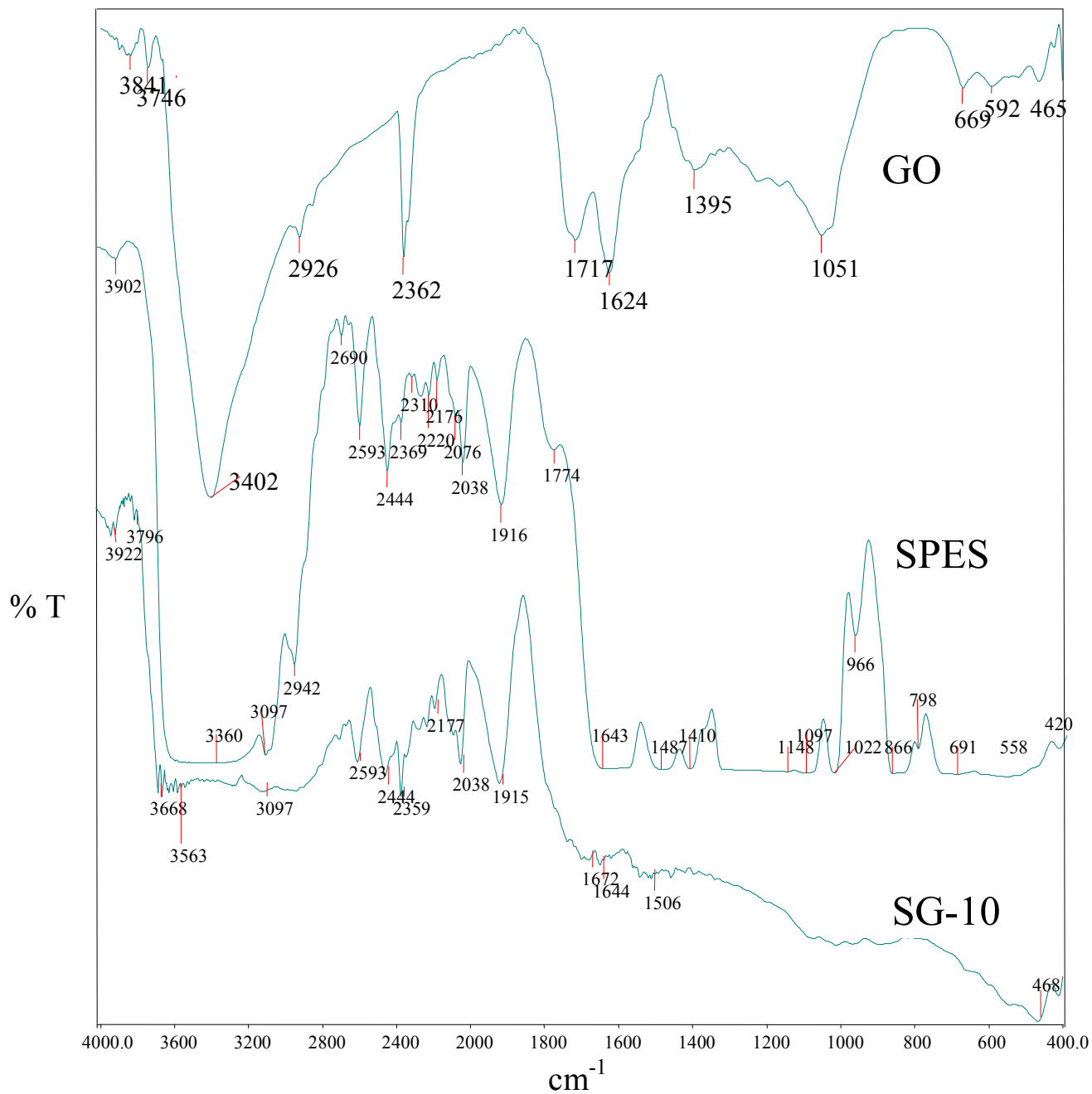


Fig. 2: FTIR spectra of GO, SPES and SG-10 Membrane

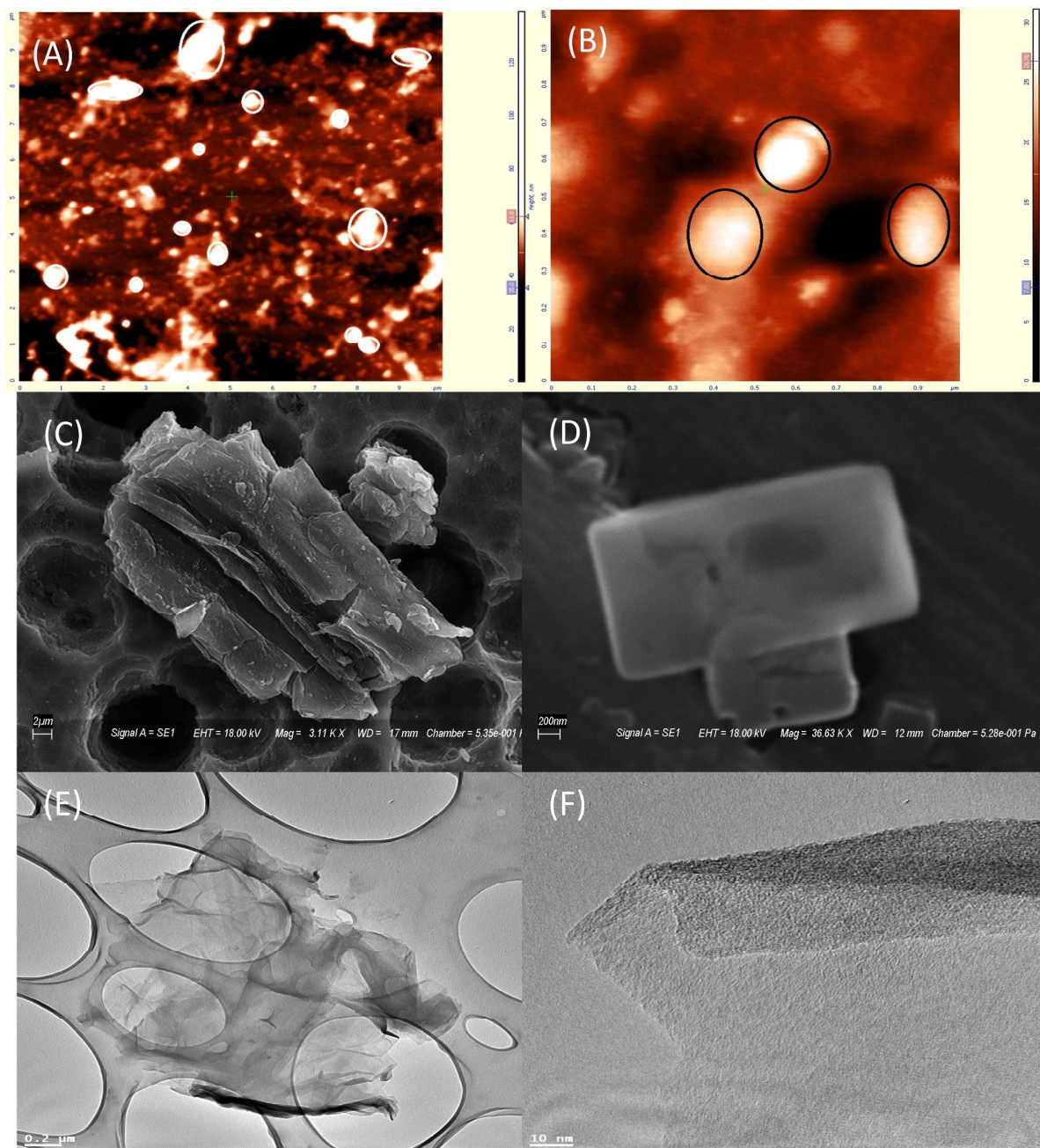


Fig. 3: AFM (A, B), SEM (C, D) and TEM (E, F) images of Graphene Oxide at different magnifications.

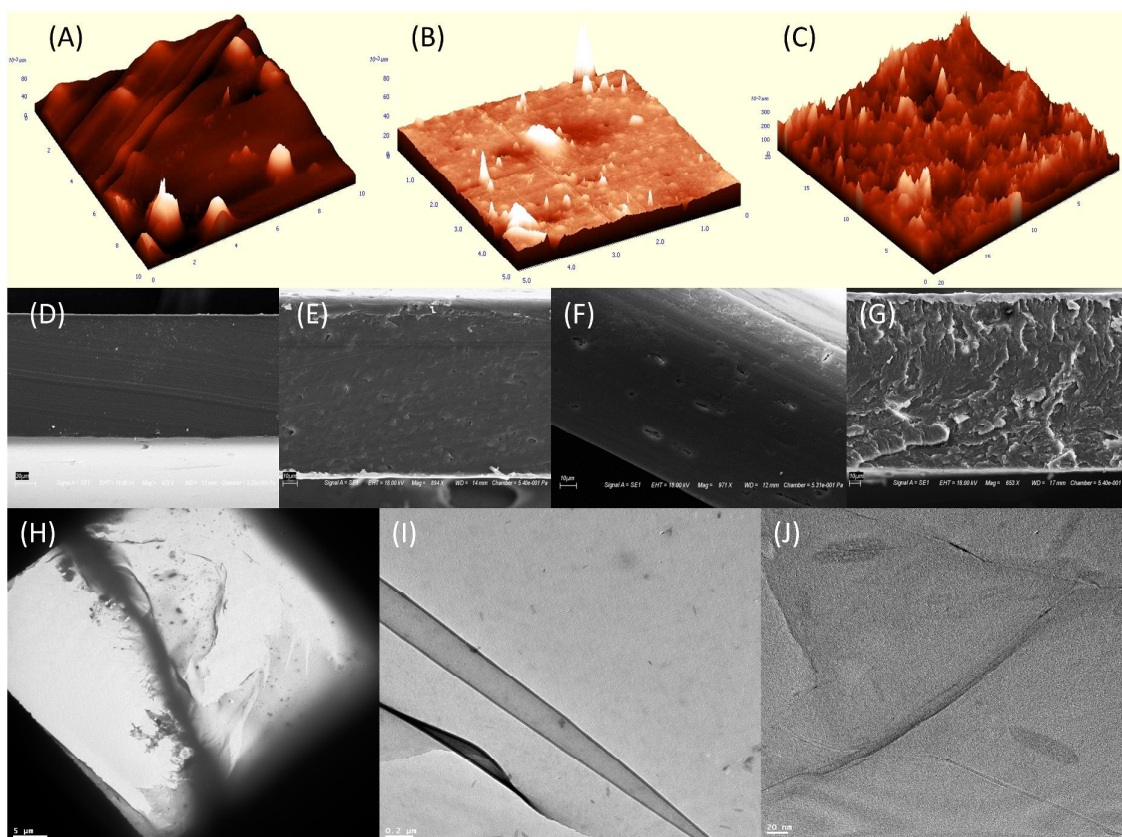


Fig. 4: AFM images of (A) SPES (B) SG-1 (C) SG-10, SEM images of (D) SPES (E) SG-1 (F) SG-5 (G) SG-10 and TEM images (H), (I), (J) of Graphene Oxide/SPES composite at different magnifications.

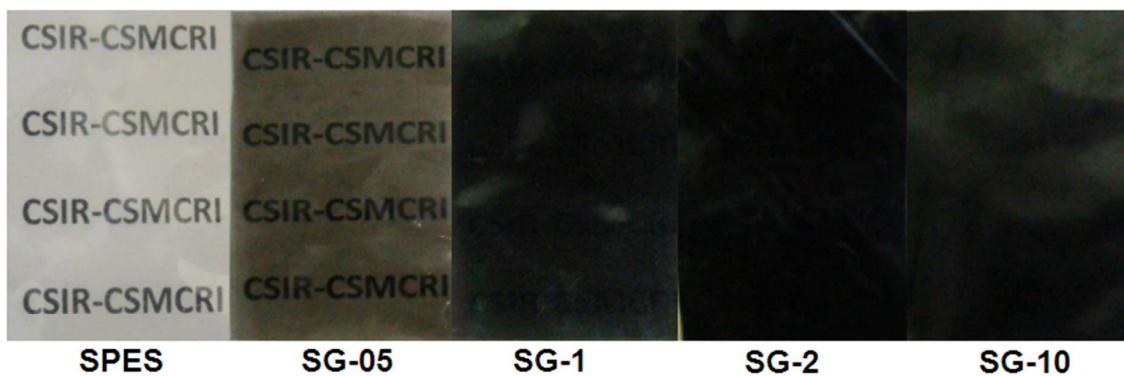


Fig. 5: Photograph of SPES and different composite membranes

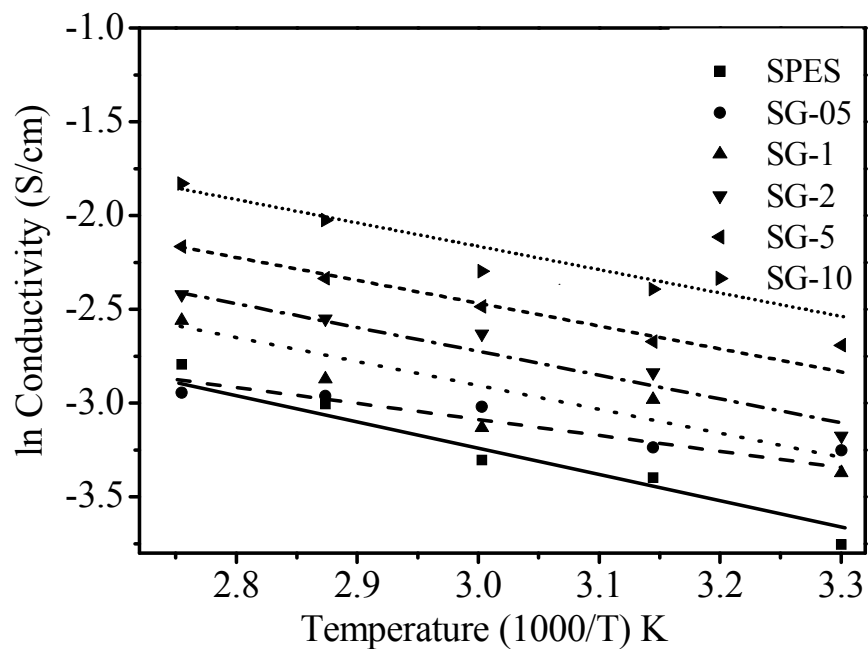


Fig. 6: Arrhenius plot of conductivity vs. temperature for different membranes

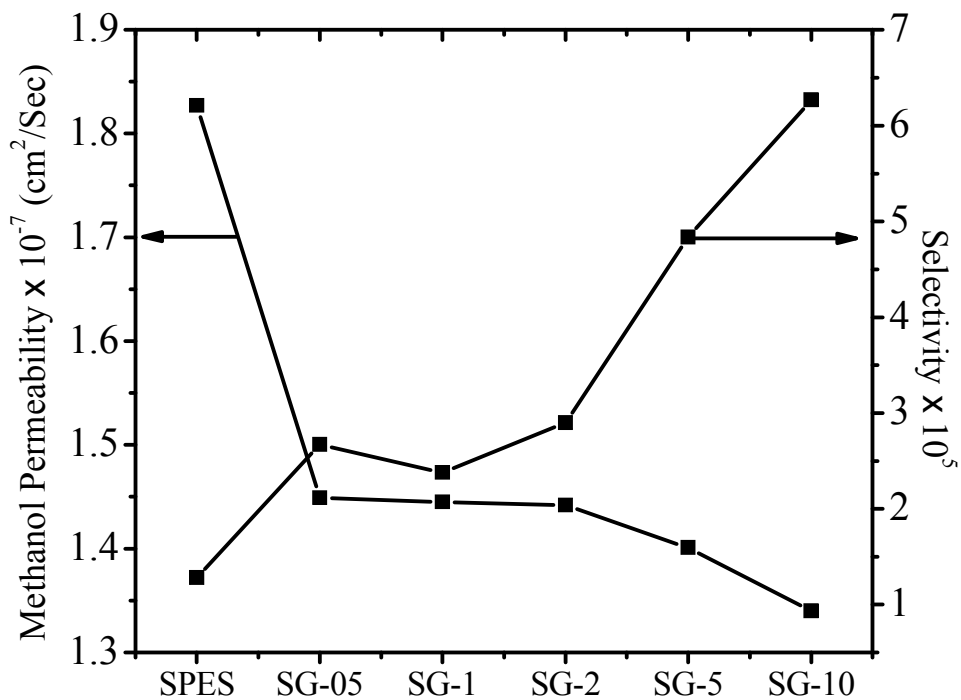


Fig. 7: Methanol permeability (P_M) and selectivity (S_p) for different membranes

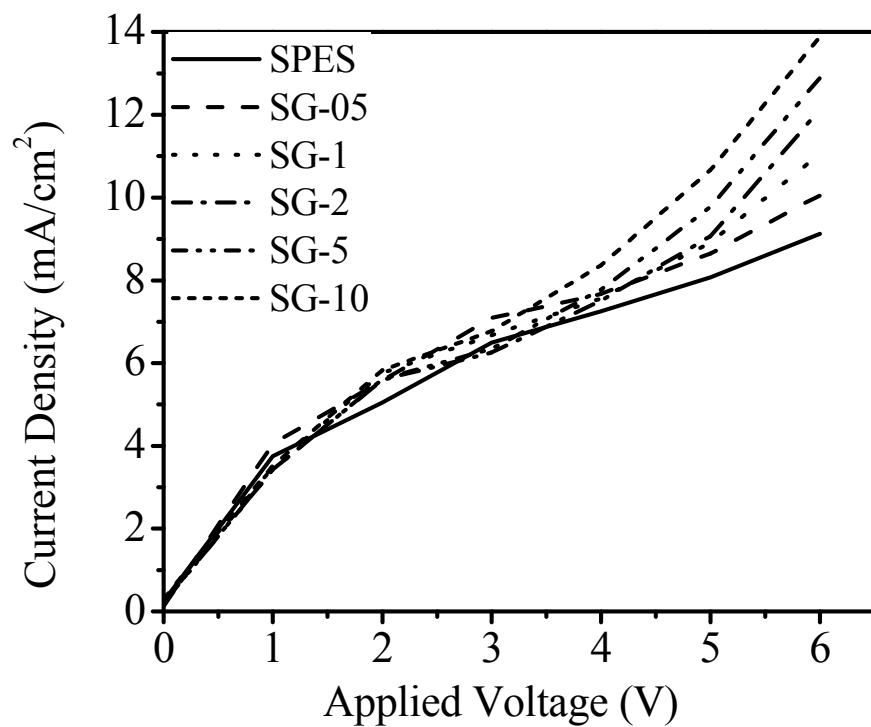


Fig. 8: Current -voltage (I-V) curve for different membranes

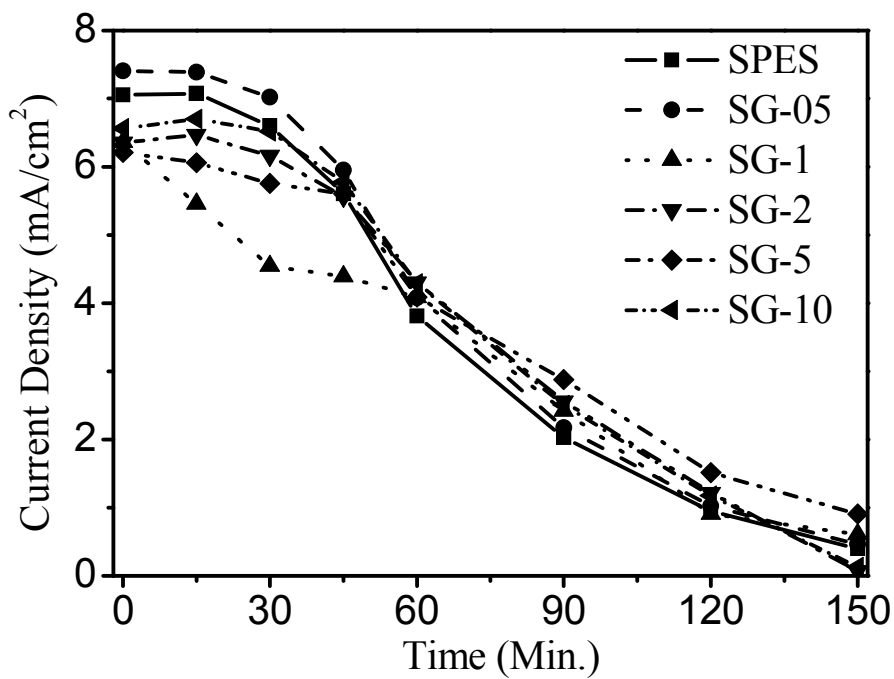


Fig. 9 (A): Time -current curve for different membranes

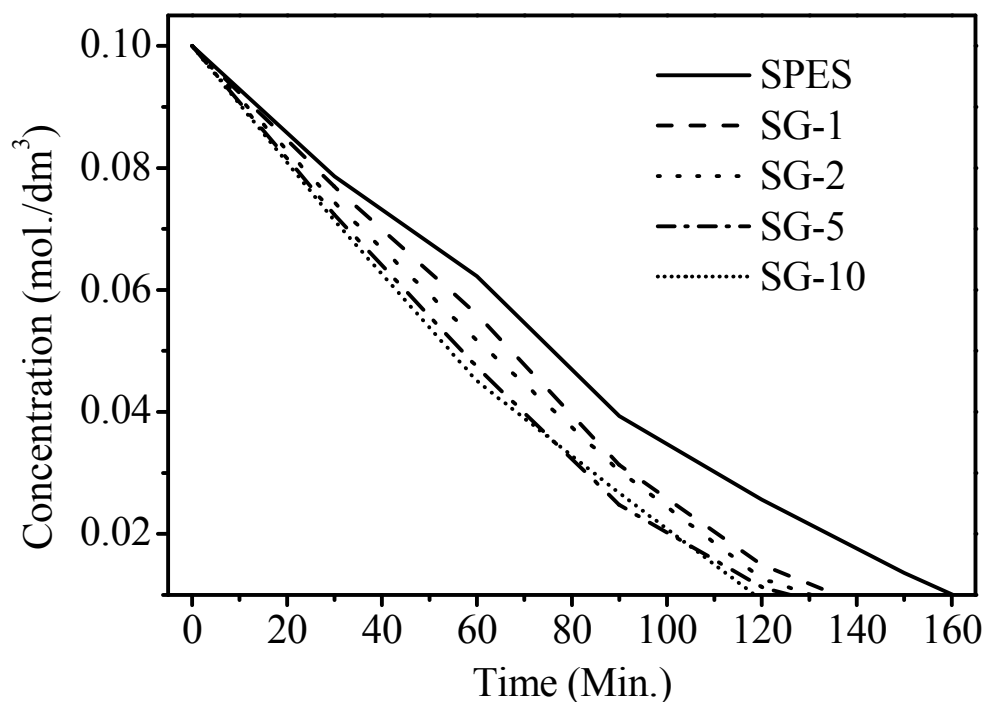


Fig. 9(B): Changes in salt concentration during electro dialysis experiment

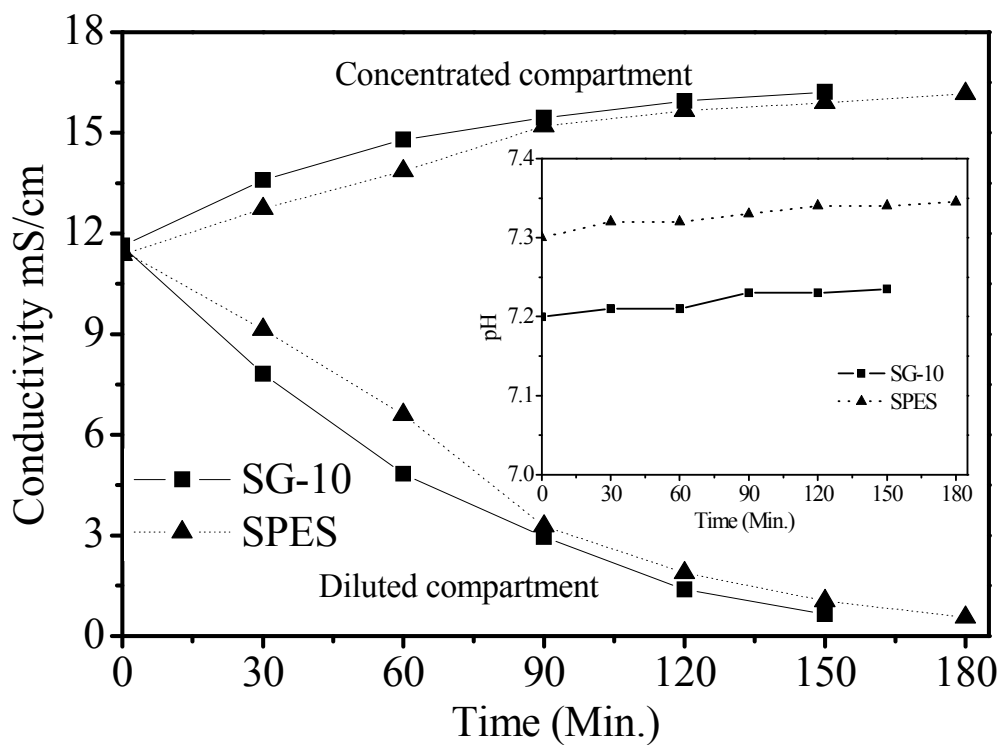


Fig. 9(C): Changes in conductivity of C.C. and D.C. and pH during electro dialysis experiment

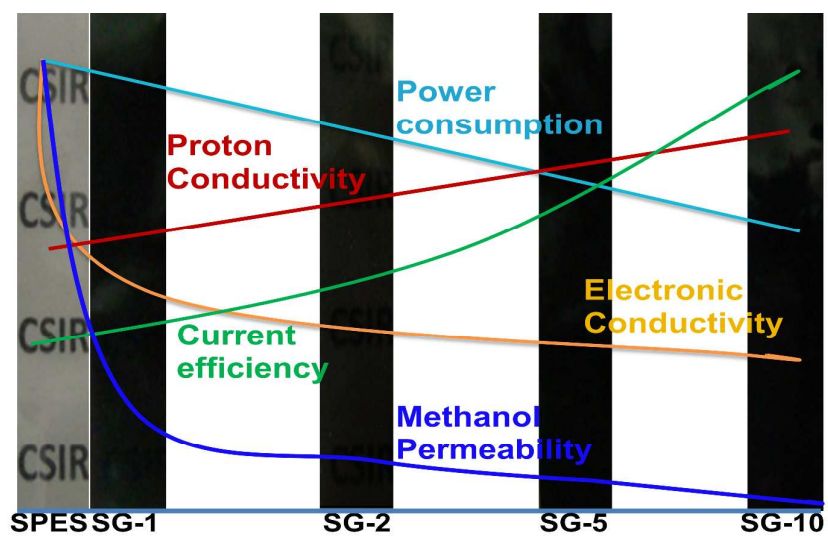


Fig. 10: Different membrane properties by inclusion of GO content

Table 1: Ion exchange capacity (IEC), water uptake (%), counter ion transport number (t_m), bound and free water (%), dimensional stability, ionic conductivity and electronic conductivity for different membranes

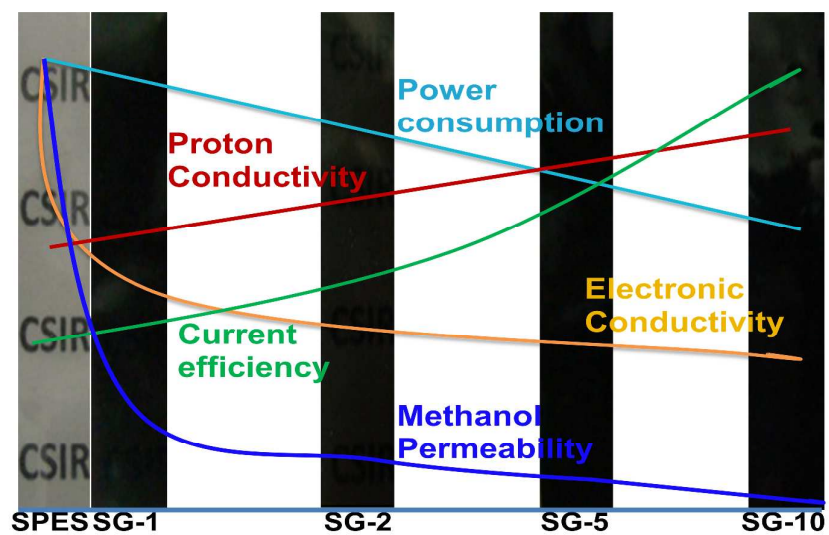
Membrane Type	IEC (meq/gm)	Water uptake %	Transport number (t_m)	Bound water %	Free Water %	Dimensional Change %	Ionic Cond. x 10^{-2} (S/cm)	Electronic Cond. x 10^{-2} (S/cm)
SPES	1.40	12.12	0.87	0.32	11.8	19.54	2.34	2.544
SG-05	1.395	13.62	0.90	0.20	13.42	16.18	3.87	0.612
SG-1	1.39	12.20	0.91	0.10	12.10	12.52	3.435	0.416
SG-2	1.37	13.71	0.93	0.67	13.04	4.55	4.177	0.177
SG-5	1.334	13.87	0.93	0.46	13.41	6.28	5.772	0.084
SG-10	1.27	15.19	0.96	0.64	14.55	7.55	6.4	0.051

Table 2: ΔV , Δi and I_{lim} values for different membranes calculated from Fig. 8.

Membrane	ΔV (V)	Δi (mAcm $^{-2}$)	I_{lim} (mAcm $^{-2}$)
SPES	3.10	2.67	5.20
SG-1	3.11	3.11	5.85
SG-2	3.34	4.72	6.20
SG-5	3.61	4.84	6.30
SG-10	3.73	4.39	6.39

Table 3: Desalination performance of different prepared membranes

Membrane Type	Flux/mole m $^{-2}$ h $^{-1}$	η	P/kW h kg $^{-1}$ salt
SPES	2.94	87.1	5.40
SG-1	3.27	91.0	4.85
SG-2	3.42	91.8	4.60
SG-5	3.51	93.7	4.44
SG-10	3.71	97.4	4.30



Different membrane properties by inclusion of Graphene oxide content